Sedimentary Geology 305 (2014) 58–68

Contents lists available at ScienceDirect

Sedimentary Geology

journal homepage: www.elsevier.com/locate/sedgeo

Magnesium isotopes in high-temperature saddle dolomite cements in the lower Paleozoic of Canada

Denis Lavoie [a,*], Simon Jackson [b], Isabelle Girard [b]

[a] Natural Resources Canada, Geological Survey of Canada, Quebec Division, 490 de la Couronne, Quebec City, QC G1K 9A9, Canada
[b] Natural Resources Canada, Geological Survey of Canada, Central Canada Division, 601 Booth Street, Ottawa, ON K1A 0E8, Canada

ARTICLE INFO

Article history:
Received 19 December 2013
Received in revised form 14 March 2014
Accepted 16 March 2014
Available online 24 March 2014

Editor: B. Jones

Keywords:
Mg isotopes
Hydrothermal dolomites
Paleozoic
Canada

ABSTRACT

Mg isotopes are used to better understand the genesis of hydrothermal saddle dolomite cements in Lower Paleozoic successions in Canada. These cements occur in fault-bounded dolostones that overlay lithologically diverse basement rocks; Ordovician dolomite lies over the Precambrian craton, whereas the Silurian and Devonian dolomites overlay a succession of tectonically accreted sedimentary, volcanic and ultramafic units of Cambrian to Ordovician age.

Lower Silurian saddle dolomites have the most negative $\delta^{26}Mg_{DSM3}$ values of our dataset (−3.25 to −1.13‰), and plot in two distinct groups: a strongly negative subset that characterizes higher temperature (175 °C) dolomites, and a less negative subset for lower temperature (153 °C) dolomites. Upper Ordovician saddle dolomites precipitated at significantly lower temperatures (102 °C), and their $\delta^{26}Mg_{DSM3}$ values range from −1.26 to −0.71‰. Lower Devonian saddle dolomites formed at very high temperature (350 °C) and have $\delta^{26}Mg_{DSM3}$ values ranging from −1.29 to −0.78‰.

No experimental data on high temperature (100–350 °C) fluid-dolomite Mg isotope fractionation factors have been published, and recent research suggests that no significant fractionation occurs between diagenetic fluids and dolomites at high temperatures in closed to semi-closed diagenetic systems. Our results indicate that the isotopic signature of diagenetic fluid is the primary control for the $\delta^{26}Mg_{DSM3}$ values in these high-temperature dolomites.

1. Introduction

Dolomites and dolomitization have been major research themes since the first scientific description of dolomite by de Dolomieu (1791). Since then, multiple hypotheses for the origin of dolomite have been proposed (van Tuyl, 1914; Hsu, 1966; Machel and Mountjoy, 1986; Machel, 2004; among others). Current models include syn-sedimentary bacteria-mediated precipitation (van Lith et al., 2002; Zhang et al., 2013), marine–meteoric water mixing (Humphrey and Quinn, 1989), shallow burial reflux (Jones and Xiao, 2005), deep burial thermo-chemical sulphate reduction (Machel, 1987) and fault-controlled hydrothermal dolomitization (Davies and Smith, 2006). Dolomite precipitation and dolomitization of precursor carbonates can result from more than one process. Nevertheless, researchers using similar data can arrive at very different conclusions (Humphrey and Quinn, 1989, 1990; Machel and Mountjoy, 1990). Apart from academic interest, an understanding of dolomitization processes is critical because dolostones are one of the most prolific hosts of the world's conventional reserves of hydrocarbons (Braithwaite et al., 2004). The mechanisms of dolomitization have been studied using multiple approaches and techniques, and recent studies incorporate a variety of petrographic (conventional, fluid inclusion microthermometry, cathodoluminescence, UV-excited light, and scanning electron microscopy) and geochemical (major-trace elements, REE, oxygen and carbon stable isotopes, strontium radiogenic isotopes, and ion chemistry of fluid inclusions) approaches in addition to detailed field or core description.

The emergence of new metal isotope systems provides a supplementary tool to better appreciate the various origins of dolomites. The understanding of Mg-isotope values in carbonates is progressing rapidly, with recent contributions on magnesium cycling in deep sea marine sediments (Higgins and Schrag, 2010), on biotic (Hippler et al., 2009) and abiotic (Immenhauser et al., 2010; Li et al., 2012) low-temperature precipitation of Mg-rich calcites and the effects of growth rates on Mg-fractionation factors in low temperature Mg-calcite (Mavromatis et al., 2013). Research on Mg-isotope behaviour in high temperature dolomites is restricted to the detailed studies of an initially

* Corresponding author. Tel.: +1 418 654 2571.
E-mail address: Denis.Lavoie@NRCan.gc.ca (D. Lavoie).

http://dx.doi.org/10.1016/j.sedgeo.2014.03.002
0037-0738/

semi-closed diagenetic system to the late open diagenetic system of Geske et al. (2012) and Azmy et al. (2013), largely based on replacement dolomites.

Here, we focus on trends in Mg isotopes for geologically and geochemically well-characterized, high temperature saddle dolomite cements in Lower Paleozoic Canadian strata (Ordovician, Silurian and Devonian). Mg-isotope values ($^{25}Mg/^{24}Mg$ and $^{26}Mg/^{24}Mg$) of these dolomites are evaluated for their potential for characterizing and contrasting sources of diagenetic fluids and aid in the assessment of Mg-sources for dolomitization.

We restrict our samples to pore- and fracture-filling saddle dolomite cements; this is done in order to minimize the additional complexity of buffering of $\delta^{25}Mg$ and $\delta^{26}Mg$ values with the Mg-isotope signatures of precursor carbonates (Geske et al., 2012; Azmy et al., 2013). The key aims of this study are: 1) to determine whether Mg-isotope values of saddle dolomite cements relate to the temperature of precipitation or to the composition of the diagenetic fluids and 2) to evaluate if Mg-isotope signatures of saddle dolomites are in agreement with the previous interpretations of the nature of hydrothermal fluids responsible for their precipitation.

2. Geological setting

The Lower Paleozoic succession of eastern Canada belongs to two major tectonostratigraphic domains (Fig. 1; Lavoie, 2008): 1) the Cambrian–Ordovician shallow marine platform and adjacent slope and rise successions (St. Lawrence Platform and Humber Zone, respectively) and 2) the Silurian–Devonian shallow to deep marine basin (Gaspé Belt). These host a large number of dolomite-rich units (Lavoie, 2008) and recent field, petrographic and geochemical works on these dolostones have led to the proposition that there are significant hydrothermal imprints on some (Table 1).

2.1. Hydrothermal dolomite occurrences and petrography

2.1.1. Upper Ordovician foreland carbonate ramp

The Upper Ordovician Taconian foreland carbonate ramp in eastern North America is known as the Trenton–Black River (TBR) interval from which hydrothermal dolomite was initially recognized as a major hydrocarbon exploration target (Hurley and Budros, 1990). These units recorded high temperature hydrothermal events in southern Quebec (TBR, Lavoie et al., 2009), Anticosti Island (Mingan Formation; Lavoie and Chi, 2010) and Hudson Bay (Red Head Rapids Formation; Lavoie et al., 2011).

The Deschambault Formation (Trenton Group) is characterized by initial calcite cementation that commonly fills most of available primary pore space. Replacement dolomitization initiated before the onset of stylolitization and continued afterwards, and the replacement dolomite occurs near small fractures that cut through the limestone facies. The replacement dolomite consists of sub-mm (0.01 to 0.15 mm) crystal size of planar-e type (Sibley and Greg, 1987), dull reddish to non-luminescence under CL (Fig. 2A, B). Saddle dolomite cements are found coating small fracture walls and within secondary dissolution pore space, the dolomite is subhedral to euhedral, planar to saddle, and 0.1 to 0.8 mm in crystal size; it is very dull reddish orange luminescent with fine very dull luminescent crystal tips (Fig. 2A, B). A late calcite phase fills most of the remaining void spaces and locally, sphalerite is observed as the last diagenetic phase.

2.1.2. Lower Silurian foreland carbonate ramp

The Lower Silurian peritidal carbonate ramp of the Gaspé Belt, comprising the Sayabec and La Vieille formations, evolved during the inception of the Acadian foreland basin (Lavoie, 2008). Locally, the carbonate ramp succession contains extensive dolostone bodies where dextral strike-slip faults juxtapose the carbonates with the Ordovician ultramafic and mafic volcanic rock units in the northern Gaspé and northern New Brunswick. Detailed field, petrographic and geochemical studies support the hydrothermal origin of these dolomites (Lavoie and Chi, 2001; Lavoie and Morin, 2004; Lavoie and Chi, 2006, 2010). Previous work on the Lower Silurian Sayabec Formation dolostones suggests that diagenetic fluids differed in composition among the western and central Gaspé locations (Table 1).

In the intensively dolomitized outcrops of the Sayabec Formation, matrix-replacive dolomite that consists of interlocking, 0.05 to 0.5 mm dolomite rhombs form the groundmass of all samples (Lavoie and Morin, 2004). The fine-grained groundmass dolomite is locally corroded at the margin of some mm- to cm-sized dissolution vugs and fractures. Pore-filling coarsely crystalline saddle dolomite lines the walls of the secondary pores. The saddle dolomite can entirely fill some small pores and fractures although, in most cases, it partially fills the largest pores. This dolomite consists of 0.5 to 2 mm, inclusion-rich euhedral to subhedral saddle crystals (Fig. 2C, D). Under CL, the crystals are red luminescent with common sub-mm non-luminescent tips (Fig. 2C, D). In some larger pores, calcite cements overlie the saddle dolomite; the calcite consists of anhedral crystals.

2.1.3. Lower Devonian pinnacle reefs

Lower Devonian pinnacle reefs of the West Point Formation in the northern Gaspé grew in response to rapid sea level rise (Bourque et al., 1986). One of these pinnacles is exposed at the junction of two major dextral transpressive faults where magmatic activity and high heat flux are recorded (Pinet et al., 2008). The pinnacle is intensively dolomitized; early saddle dolomite records very high precipitation temperatures, with homogenization temperatures of primary fluid inclusions ranging between 301 and 382 °C. Petrographic and geochemical data suggest a major hydrothermal imprint on the carbonate facies (Lavoie et al., 2010).

The massively dolomitized section of the West Point Formation contains three phases of dolomite as well as a late calcite phase; the second phase of saddle dolomite has been analysed for its Mg isotope values. The first dolomite phase is rare (volumetrically less than 1%) and consists of anhedral crystals that range in size from 0.005 to 0.05 mm (0.0002 to 0.002 in). The second dolomite is the most abundant phase in the pinnacle reef, making up over 90% of the total rock volume; it is represented by euhedral, iron-rich crystals that range from 0.5 to 8 mm (0.02 to 0.3 in) in size (Fig. 2E, F). This pore-filling dolomite is dull red luminescent. The last saddle dolomite is restricted to fractures cutting through the pinnacle and makes up roughly 5% of the total rock volume.

3. Interpretation of hydrothermal fluids from geochemical tracers

Based on the data available from the previous studies (Table 1), we provide some interpretations as to the origin of the hydrothermal fluids responsible for the precipitation of saddle dolomites in the Upper Ordovician, Lower Silurian and Lower Devonian dolostones. More details can be found in the above-cited literature. $\delta^{18}O_{VSMOW}$ values of the dolomitizing fluids can be determined from fluid inclusion homogenization temperatures (T_h) and $\delta^{18}O_{VPDB}$ value of the same dolomite crystal (Table 2 and Fig. 2); the stable isotope fractionation between dolomite and water has been calculated using Zheng's (1999) equation. The data indicate that the Upper Ordovician, Lower Silurian (western Gaspé), and Lower Devonian saddle dolomites precipitated over a wide range of temperatures from ^{18}O-enriched brines (+4 to +12‰) with the Upper Ordovician examples being slightly less enriched. Lower Silurian saddle dolomites from central Gaspé precipitated from a near marine fluid (−1 to 0.8‰).

Calculated fluid $\delta^{18}O_{VSMOW}$ values and $^{87}Sr/^{86}Sr$ ratios of saddle dolomite samples (Fig. 3) suggest that Upper Ordovician saddle dolomites are more radiogenic that contemporaneous seawater (Denison et al., 1997; Shields et al., 2003). Lower Silurian saddle dolomite parent fluid

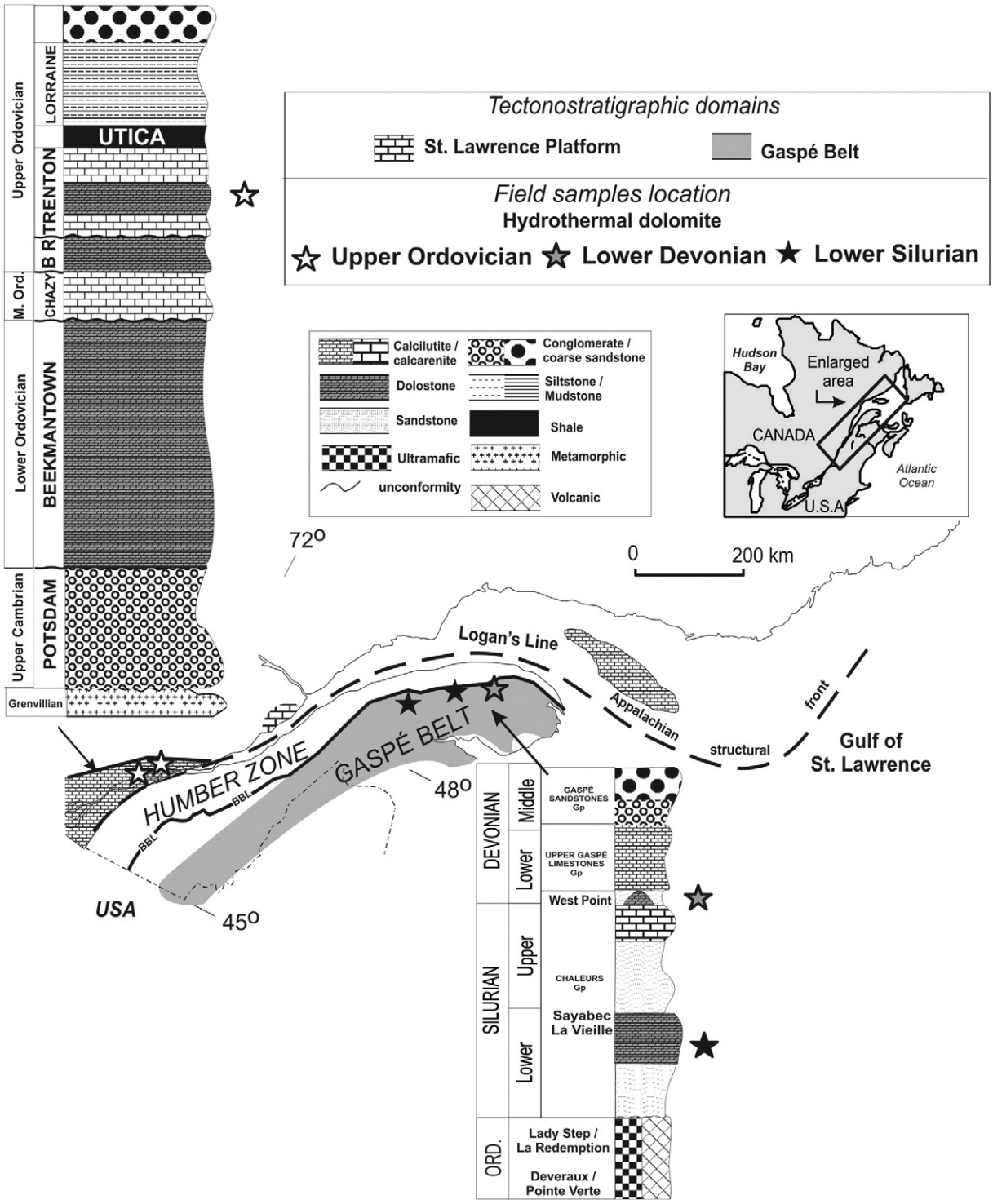

Fig. 1. Geological map of southern Quebec (eastern Canada) with the location of the Cambrian–Ordovician St. Lawrence Platform and Humber Zone, and the Silurian–Devonian Gaspé Belt. Location of samples is shown with stars. Two stratigraphic columns present the general stratigraphic framework of this area with the stratigraphic location (stars) of sampled dolostones. Geology and stratigraphic sections modified from Lavoie (2008).

$\delta^{18}O_{VSMOW}$ values comprise two fields that differ in their Sr-isotope values; western Gaspé samples are more radiogenic than Early Silurian seawater (Denison et al., 1997) whereas those from central Gaspé are similar to the Early Silurian $^{87}Sr/^{86}Sr$ seawater value (Denison et al., 1997). No samples for Lower Devonian saddle dolomites have paired $^{87}Sr/^{86}Sr$ and $\delta^{18}O_{VSMOW}$ values; however, three samples of the high temperature dolomite have $^{87}Sr/^{86}Sr$ values (0.708383 to 0.709216; Lavoie et al., 2010) that compare well with the average seawater value for Early Devonian seawater (0.70870; Denison et al., 1997).

With the exception of Lower Devonian examples, saddle dolomite fluid inclusions are highly saline (Table 1). Based on first melting temperatures (−70 to −50 °C), Lavoie et al. (2005) have proposed that the brine responsible for the precipitation of saddle dolomite in the Lower Ordovician Romaine Formation of Anticosti Island (not studied

Table 1
Summary of stable and radiogenic isotope data and microthermometric fluid inclusion data for saddle dolomite occurrences in the Lower Paleozoic of eastern Canada. U.O.: Upper Ordovician, L.S.: Lower Silurian, L.D.: Lower Devonian. N is for number of analyses. N/A is for not available.

Unit	$\delta^{18}O_{PDB}$ ‰ (mean)	$\delta^{13}C_{PDB}$ ‰ (mean)	T_h °C (mean)	Salinity wt.%$NaCl_{equi.}$ (mean)
Trenton (U.O.)	−11 to −4.5 (−9.8) 2σ: 1.6 N: 11	−2.5 to 2 (−0.3) 2σ: 1.6 N: 11	85–128 (102) 2σ: 10.5 N: 16	22.8–24.7 (23.8) 2σ: 0.6 N: 13
Red Head Rapids (U.O.)	−17.4 to −10.3 (−14.2) 2σ: 1.8 N: 12	−8.3 to −1.4 (−3.9) 2σ: 1.7 N: 12	N/A	N/A
Sayabec (L.S.)				
Central Gaspé	−17.9 to −16.9 (−17.0) N: 3	−1.6 to −0.3 (−0.5) N: 3	111–194 (153) 2σ: 19 N: 44	21.1–28 (23) 2σ: 1.5 N: 21
Western Gaspé	−15.3 to −6.7 (−10.5) 2σ: 3.5 N: 6	−3.5 to 3.3 (0) 2σ: 2.8 N: 6	140–218 (175) 2σ: 23 N: 6	22.5−24.8 (23.2) 2σ: 0.3 N: 4
La Vieille (L.S.)	−17.3 to −9.9 (−13.9) 2σ: 2.7 N: 5	−2.6 to 1.3 (−0.4) 2σ: 1.4 N: 5	N/A	N/A
West Point (L.D.)	−19.1 to −15.8 (−17.2) 2σ: 0.9 N: 7	−7.9 to −1.4 (−3.1) 2σ: 2.2 N: 7	301–382 (350) 2σ: 15.5 N: 36	6.9–17.3 (13.3) 2σ: 1.9 N: 36

here) had a non- or significantly altered-marine $MgCl_2$–$CaCl_2$–NaCl composition. Similar brines have been recognized in coeval successions (Lower Ordovician St. George Group; Conliffe et al., 2009, 2010) and in the Lower Silurian La Vieille Formation (Lavoie and Chi, 2006).

Based on diverse $\delta^{18}O_{VSMOW}$, $^{87}Sr/^{86}Sr$ and salinity values, very distinct fluids were responsible for the precipitation of high temperature saddle dolomite cements in these Lower Paleozoic successions.

4. Methods

4.1. Sampling of saddle dolomite

The sampling of the saddle dolomite cements was made with a Jansen micro-sampler. Polished rock blocks were examined and photomicrographed, together with the associated thin sections, under a cold cathodoluminoscope (Nuclide). Samples were micro-drilled from parent rock slabs and homogeneity of cement samples was confirmed through CL examination of milled areas.

4.2. Reagents

Trace metal grade HNO_3, HCl, $HClO_4$, and HF were used for the digestion of samples in PTFE beakers, and digested samples were stored in HDPE centrifuge tubes, pre-washed for 24 h in 4 M trace metal grade HCl and rinsed with Milli-Q water prior to use. Ultra-pure HCl and HF from Seastar were used to prepare the chromatography eluants, while acetone was purified in-house by sub-boiling distillation. The HCl used to dilute the samples was also the ultra-pure grade from Seastar and the water used in all procedures was ≥18 MΩ from a Millipore Milli-Q system. Chromatography was performed in poly-prep columns using AG50-X8 resin, both from BioRad.

4.3. Digestion

Twenty to 50 mg of sample was digested in two batches of approximately 25 samples with 10 mL of 6 N HNO_3 at room temperature for 24 h. Each sample was transferred to a 50 mL HDPE centrifuge tube, brought up to 25 mL with Milli-Q water, shaken and then centrifuged. Each batch contained one blank. Dolomite reference materials NBS-88a (NBS) and JDo-1 (GSJ) were prepared along with the samples.

4.4. Chromatography

All digested samples were analysed on a Perkin Elmer Optima 3000 ICP-OES to determine the concentration of all major and many trace elements. Magnesium was separated following the protocol described in Wombacher et al. (2009), involving two elutions on 1 mL of AG50W-X8 resin. Two elutions were used because many samples contain high concentrations of Ca, which is known to cause matrix effects on the Mg-isotope values (Galy et al., 2001). This approach allows the separation of most of the Ca from Mg in the first elution, ensuring complete separation of Mg from any residual Ca during the second elution.

Care was taken to verify that the protocol was suitable for all types of samples involved in this study and related, more wide-ranging investigations by running synthetic solutions containing major elements (Ca, K, Mg, Fe, Al, and Ti) in the range of concentrations observed in the samples. To ensure that 100 ± 2% recovery of Mg was achieved, Mg fractions obtained from reference materials DSM3 (Galy et al., 2003), NBS88a, UB-N (serpentine, CRPG), BCR-2 (basalt, USGS) and DTS-1 (dunite, USGS) were analysed by ICP-OES. Magnesium recoveries ranged from 98.6 to 99.9%, all other major elements determined were at less than their detection limits (ca. 0.1 ppm; c.f. Mg concentrations ranging from 10 to 75 ppm). An aliquot of the DSM3 Mg-isotope reference standard (Galy et al., 2003) was also run through the resin to verify that the chromatography protocol did not induce fractionation of Mg.

Total milli-equivalent grammes per millilitre of Mg and matrix elements (Ca + K + Fe + Na + Ti + Al + Mn) were calculated from the elemental analysis, and the determined volume of each sample containing 0.48 milli-equivalent grammes of Mg and matrix elements, representing 40% of the maximum resin capacity, was brought down to dryness, then picked up in 1 mL of 10 M HCl to achieve a solution suitable for chromatography. Depending on sample composition, between 10 and 250 μg of Mg were purified. Column blanks were prepared by processing 1 mL of Seastar 10 M HCl.

4.5. Instrumental

Magnesium-isotope ratios of samples, blanks and reference materials were determined on a Nu Plasma double-focusing multi-collector ICP-MS from Nu Instrument in low resolution. The instrument is equipped with twelve fixed Faraday detectors and three ion counters. Faraday cups used were L5, Axial and H6 for ^{24}Mg, ^{25}Mg and ^{26}Mg respectively, with a mass separation of 0.125 amu. A desolvating nebulization system (DSN) was used for sample introduction, with a 'micro-mist' nebulizer operated at a 100 μL/min flow rate. The use of the DSN, in conjunction

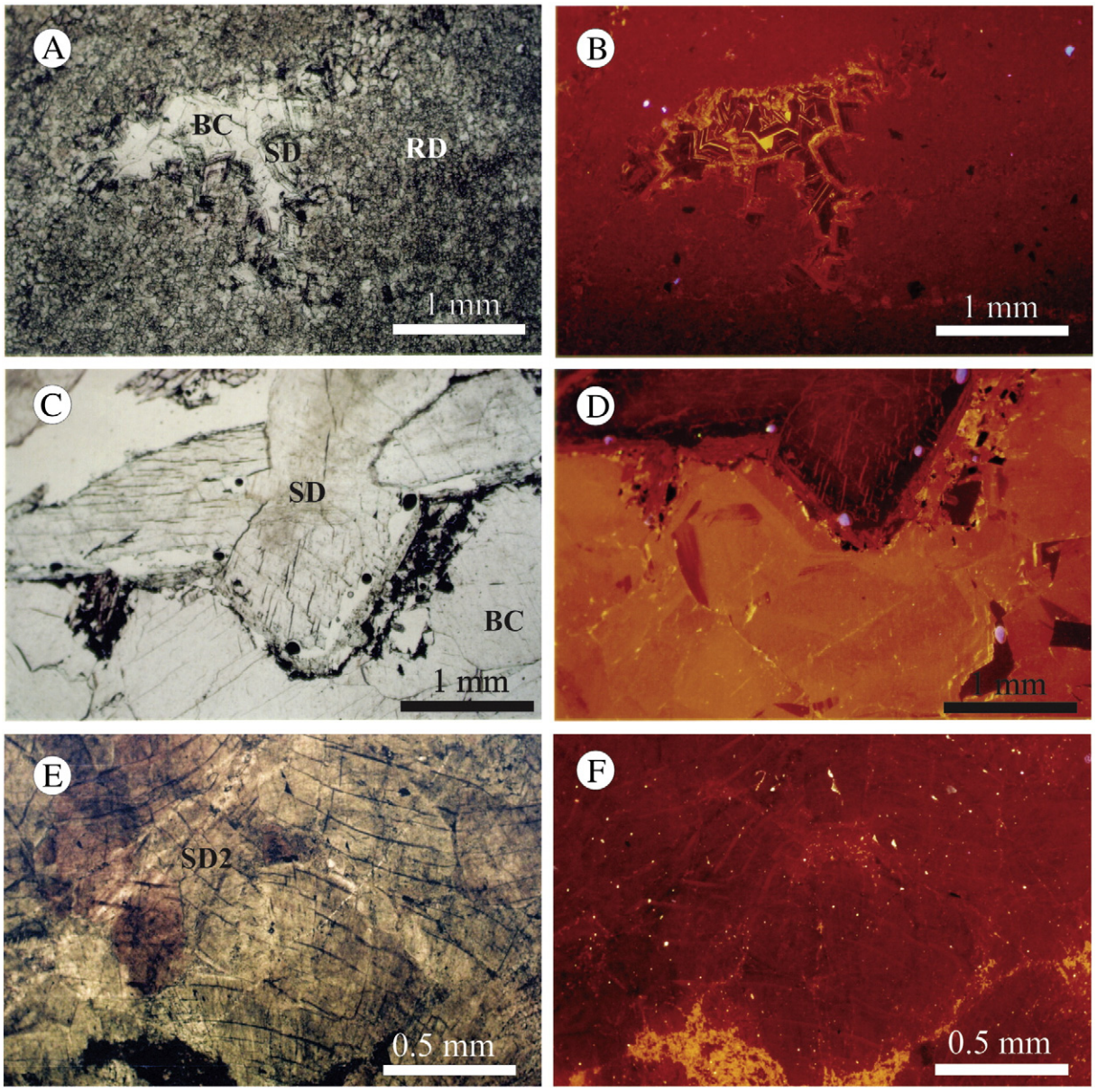

Fig. 2. Paired photomicrographs in plane polarized light and under cathodoluminescence of saddle dolomite cements for the three studied units. A and B, Upper Ordovician Deschambault Formation (Trenton Group). C and D, Lower Silurian Sayabec Formation. E and F, Lower Devonian West Point Formation. SD is saddle dolomite, RD is replacive dolomite, and BC is burial calcite.

with diluting in HCl rather than HNO_3, reduced the $^{12}C^{14}N^{+}$ interference on ^{26}Mg to insignificant levels (undetectable in a high resolution scan across the ^{26}Mg peak) and no actions beyond measuring an on-peak zero were taken to correct for it. It was found that the $^{12}C^{+}$ dimer interference on ^{24}Mg could also be kept to insignificant levels by cleaning the sampler cone daily. Ion lens voltages and the membrane gas flow on the DSN were optimized daily.

The final magnesium fraction of the samples, reference materials and reference calibration standard, DSM3, were diluted in 0.12 M HCl for instrumental analysis to obtain a minimum signal of 4 V on ^{24}Mg, but no more than 7 V. The concentration was typically 75 ppb Mg. Once the ^{24}Mg signal intensity for DSM3 was established on any day, care was taken to ensure that samples were diluted to match this signal to within a 10% tolerance.

Analysis was performed using the sample-standard-bracketing (SSB) technique and on-mass zero measurement. Zero measurements were performed with an integration time of 30 s each morning after rinsing the instrument with 0.12 M HCl for at least 10 min. Samples were analysed by acquiring 40 measurements with a 5 second integration time, taken after a 30 second stabilization time and a 2-minute rinse between samples. Magnesium-isotope reference material DSM3 was used in the SSB protocol for calibrating mass bias drift, heterogeneity problems having been reported with SRM980 Mg-isotope standard (Galy et al., 2003).

Each sample, blank and SRM were analysed in triplicate by alternating between DSM3 (4 analyses) and sample (3 analyses), starting and finishing with DSM3. Results were accepted if: (1) the signal intensity of ^{24}Mg for samples and standard were within 10% (c.f. 30% of Wombacher et al., 2009), (2) both $^{25}Mg/^{24}Mg$ and $^{26}Mg/^{24}Mg$ showed no more than 0.25‰ drift from the first to the last of a group of 4 bracketing DSM3 analyses, and (3) the $\delta^{25}Mg_{DSM3}$ and $\delta^{26}Mg_{DSM3}$ of the three sample replicates fell within 0.1‰, where:

$$\delta^{2X}Mg_{DSM3} = \left(^{2X}Mg/^{24}Mg_{sample} - ^{2X}Mg/^{24}Mg_{DSM3}\right) / \left(^{2X}Mg/^{24}Mg_{DSM3}\right) \times 1000.$$

Table 2
Samples with Mg-isotope ratios for saddle dolomite cements with other geochemical and microthermometric data where available. N.A. not available.

Unit	$\delta^{18}O_{PDB}$ ‰	T_h °C mean	$\delta^{18}O_{SMOW}$ ‰	$^{87}Sr/^{86}Sr$	$\delta^{26}Mg_{DSM3}$ ‰	$\delta^{25}Mg_{DSM3}$ ‰
Trenton (Upper Ordovician)	−5.4	92 2σ: 4 N: 6	5.3	0.708815	−0.71 2σ: 0.08	−0.33 2σ: 0.06
Trenton (Upper Ordovician)	−4.5	102 2σ: 3.8 N: 3	7.5	0.709034	−0.97 2σ: 0.12	−0.5 2σ: 0.03
Trenton (Upper Ordovician)	−6.0	111 2σ: 7.6 N: 7	7.1	0.708838	−0.79 2σ: 0.2	−0.43 2σ: 0.13
Read Head Rapids (Upper Ordovician)	−12.4	N.A.	N.A.	N.A.	−1.1 2σ: 0.3	−0.7 2σ:
Read Head Rapids (Upper Ordovician)	−13.3	N.A.	N.A.	N.A.	−1.26 2σ: 0.06	−0.84 2σ: 0.04
Sayabec — West (Lower Silurian)	−7.8	194 2σ: 18 N: 3	12.1	0.709553	−2.09 2σ: 0.09	−1.08 2σ: 0.08
Sayabec — West (Lower Silurian)	−7.3	158 2σ: 16.5 N: 3	10.2	0.710105	−1.91 2σ: 0.02	−0.95 2σ: 0.08
Sayabec — Central (Lower Silurian)	−17.4	146 2σ: 19.7 N: 23	−1.02	0.708277	−1.41 2σ: 0.01	−0.73 2σ: 0.04
Sayabec — Central (Lower Silurian)	−16.9	165 2σ: 11.5 N: 22	0.86	0.708533	−1.29 2σ: 0.22	−0.71 2σ: 0.13
Sayabec — Central (Lower Silurian)	−17.9.	N.A.	N.A.	N.A.	−1.13 2σ: 0.3	−0.59 2σ: 0.18
La Vieille (Lower Silurian)	−16.2	N.A.	N.A.	N.A.	−3.25 2σ: 0.11	−1.71 2σ: 0.05
La Vieille (Lower Silurian)	−14.0	N.A.	N.A.	N.A.	−2.18 2σ: 0.08	−1.12 2σ: 0.06
West Point (Lower Devonian)	−17.1	340 2σ: 7.7 N: 16	8.2	N.A.	−0.91 2σ: 0.06	−0.42 2σ: 0.06
West Point (Lower Devonian)	−15.8	362 2σ: 21.1 N: 10	10.0	N.A.	−0.99 2σ: 0.09	−0.59 2σ: 0.05
West Point (Lower Devonian)	−19.1	354 2σ: 4.0 N: 10	6.5	N.A.	−0.78 2σ: 0.17	−0.38 2σ: 0.13
West Point (Lower Devonian)	−17.0	N.A.	N.A.	0.709199	−1.29 2σ: 0.12	−0.71 2σ: 0.09

4.6. Blanks, precision and accuracy

Repeated measurements of DSM3 were used to determine the precision of the isotope measurements. Short-term reproducibility determined from 12 measurements was 0.04‰ for $\delta^{25}Mg$ and 0.05‰ for $\delta^{26}Mg$. Long term reproducibility determined from 240 analyses of DSM3 over a period of one year was 0.11‰ for $\delta^{25}Mg$ and 0.18‰ for $\delta^{26}Mg$.

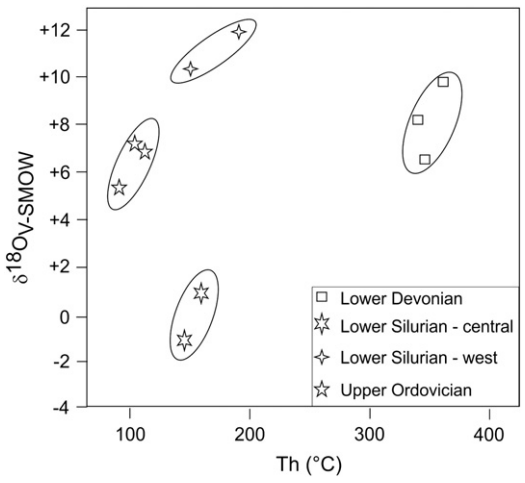

Fig. 3. Fluid $\delta^{18}O_{SMOW}$ *versus* fluid inclusion homogenization temperatures (T_h) in saddle dolomite cements. Data in Table 2.

Digestion replicates and column replicates were analysed to monitor overall uncertainty and uncertainty related to the chemical separation respectively. Table 3 presents the results obtained for replicate samples. All results agree within uncertainty.

Accuracy was assessed by analysing reference materials and comparing them to previously published results. Table 4 compares the results obtained for Cambridge-1 Mg isotopic standard and dolomite reference material JDo-1 with published values. Results agree with previously published values within uncertainty. New data are also presented for NBS88a (dolomite) and SDo-1 (shale, USGS) and reference materials.

The DSM3 standard that was processed through the column separation procedure shows that this protocol induces a bias of <0.04‰ on $\delta^{26}Mg$ and <0.002‰ on $\delta^{25}Mg$, which is well within uncertainty of the method.

Method blanks were prepared along with the samples in order to determine their impact on the isotope measurements. The blanks contained no more than 50 ng of Mg, which is <0.5% of the lowest amount of Mg loaded on the column. The impact of the blanks on the isotope measurements is <0.05‰ on $\delta^{26}Mg$ and <0.02‰ on $\delta^{25}Mg$, which is well within uncertainty of the method.

5. Results

A total of 16 pore and fracture-filling saddle dolomite cements were separated and analysed for their $\delta^{25}Mg_{DSM3}$ and $\delta^{26}Mg_{DSM3}$ values

Table 3
Magnesium isotope composition of digestion and column replicates relative to standard DSM3.

Sample	$\delta^{26}Mg_{DSM3}$	2sd	$\delta^{25}Mg_{DSM3}$	2sd
Column replicates				
08-02	−0.97	0.12	−0.50	0.03
08-02-R	−0.91	0.09	−0.48	0.11
09-03	0.09	0.09	0.05	0.07
09-03-R	0.09	0.03	0.05	0.07
2010-10	−0.11	0.12	−0.23	0.15
2010-10-R	−0.10	0.11	−0.19	0.07
2010-16	−1.29	0.22	−0.71	0.13
2010-16-R	−0.96	0.22	−0.53	0.12
Digestion replicates				
08-13	−1.91	0.02	−0.95	0.08
08-13-R	−1.84	0.11	−0.92	0.04
NBS88a	−1.76	0.03	−0.93	0.06
NBS88a-R	−1.71	0.20	−1.02	0.15

(Table 2 and Fig. 4). $\delta^{26}Mg_{DSM3}$ values for the Lower Silurian La Vieille Formation (N = 2) in New Brunswick have the most negative values of the data set (−3.25 and −2.18‰). The coeval Sayabec Formation (N = 5) of the Gaspé Peninsula is also characterized by negative $\delta^{26}Mg_{DSM3}$ values (−2.09 to −1.13‰). The Upper Ordovician dolomites (N = 5) from the Trenton Group and Red Head Rapids Formation have $\delta^{26}Mg_{DSM3}$ values that range between −1.26 and −0.71‰. The Lower Devonian West Point Formation (N = 4) have $\delta^{26}Mg_{DSM3}$ values of −1.29‰ to −0.78‰, and these values overlap those of the Ordovician dolomites (Fig. 4).

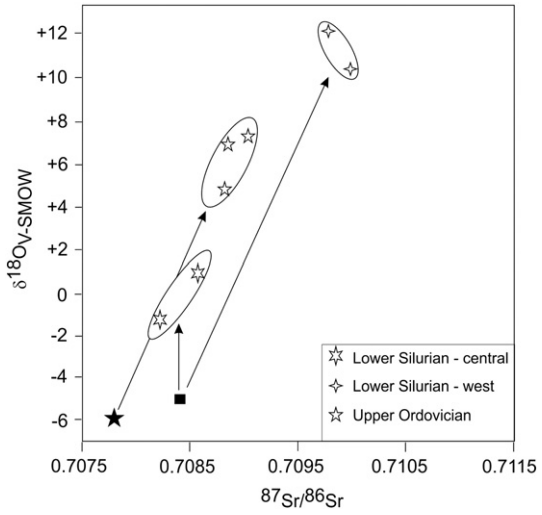

Fig. 4. Fluid $\delta^{18}O_{SMOW}$ *versus* $^{87}Sr/^{86}Sr$ values in saddle dolomite cements. The width and height of the rectangle are based on the range of values. Published inferred values of coeval seawater ^{18}O and $^{87}Sr/^{86}Sr$ shown as the black star (Late Ordovician) and square (Early Silurian). Data in Table 2.

6. Interpretation

6.1. Fluid control on Mg-isotope composition of saddle dolomites

Homogenization temperatures (T_h) from primary fluid inclusions indicate that they precipitated over a wide range of temperatures (85–382 °C; Table 1). However, many units can be distinguished on the basis of their temperature range and average (Fig. 5); the Upper Ordovician samples have the lowest average temperature (85–128 °C; mean = 102 °C, N = 16; Lavoie et al., 2010); the Lower Devonian West Point reef samples have the highest temperatures (301–382 °C; mean = 350 °C, N = 36; Lavoie et al., 2010), whereas the Lower Silurian Sayabec Formation samples have intermediate temperatures divisible on the basis of location; 111–194 °C (mean = 153 °C, N = 44) for central Gaspé (Lavoie and Chi, 2001) and 140–218 °C (mean = 175 °C; N = 23) for western Gaspé (Lavoie and Chi, 2010). In the following sections, the Lower Silurian La Vieille Formation of New Brunswick will not be discussed given the absence of microthermometric and radiogenic strontium isotope data to better constrain the diagenetic history of these samples.

$\delta^{26}Mg_{DSM3}$ values are relatively constant for a wide range of temperatures (~100 to 380 °C; Fig. 5), although the Lower Silurian samples from western Gaspé have lower $\delta^{26}Mg_{DSM3}$ values. The Mg-isotope dataset suggests that different Mg-rich fluids precipitated dolomite within units at the two Lower Silurian localities; the western Gaspé Peninsula samples record higher temperature and have more negative $\delta^{26}Mg_{DSM3}$ values (Fig. 5).

The only published data on Mg-isotope compositions of high temperature dolomites (100–350 °C) are those of Geske et al. (2012) (Triassic, southern Alps) and Azmy et al. (2013) (Lower Ordovician, eastern Canada). They suggest that there is little fluid–solid fractionation of Mg-isotopes at these temperatures under initially semi-closed to later more open diagenetic systems. The likelihood of a geochemically similar fluid for saddle dolomite precipitation in the Upper Ordovician, Lower Silurian (Central Gaspé) and Lower Devonian samples is possible; but, given the geological constraints of lithologically diverse basements and variable timing of dolomitization, this scenario seems highly unlikely.

The relation between $\delta^{26}Mg_{DSM3}$ values and calculated fluid $\delta^{18}O_{VSMOW}$ values (Fig. 6) suggests that, except for the Lower Silurian samples from western Gaspé, $\delta^{26}Mg_{DSM3}$ values are rather similar over a wide spread of $\delta^{18}O_{VSMOW}$ values. Based on their $\delta^{18}O_{VSMOW}$ values, the Lower Silurian dolomites of central Gaspé precipitated from a near marine fluid, although their $\delta^{26}Mg_{DSM3}$ values suggest a similar source of magnesium as the Upper Ordovician and Lower Devonian samples.

The relation between $\delta^{26}Mg_{DSM3}$ values and their $^{87}Sr/^{86}Sr$ ratios (Fig. 7) suggests that the Lower Silurian samples from the central

Table 4
Magnesium isotope composition of selected reference materials relative to standard DSM3.

Sample	n_s	n_m	$\delta^{26}Mg_{DSM3} \pm 2sd$	$\delta^{25}Mg_{DSM3} \pm 2sd$	$\delta^{26}Mg_{DSM3} \pm 2sd^{ref}$	$\delta^{25}Mg_{DSM3} \pm 2sd^{reference}$
Isotopic reference standard						
Cambridge-1	0	6	−2.54 ± 0.11	−1.32 ± 0.06	−2.58 ± 0.14[a]	−1.33 ± 0.07[a]
Carbonate and sedimentary rocks						
JDo-1	2	4	−2.38 ± 0.36	−1.27 ± 0.09	−2.38 ± 0.18[b]	−1.22 ± 0.07[b]
NBS88a	2	4	−1.76 ± 0.09	−0.96 ± 0.22		
SDo-1	1	2	−0.10 ± 0.08	−0.07 ± 0.03		

n_s: number of chemical separations, n_m: total number of (triplicate) measurements.
[a] Galy et al. (2003).
[b] Wombacher et al. (2009).

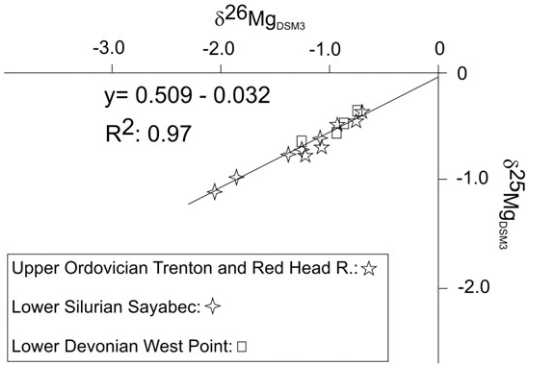

Fig. 5. $\delta^{26}Mg_{DSM3}$ *versus* $\delta^{25}Mg_{DSM3}$ for lower Paleozoic dolomite cements. Data in Table 2.

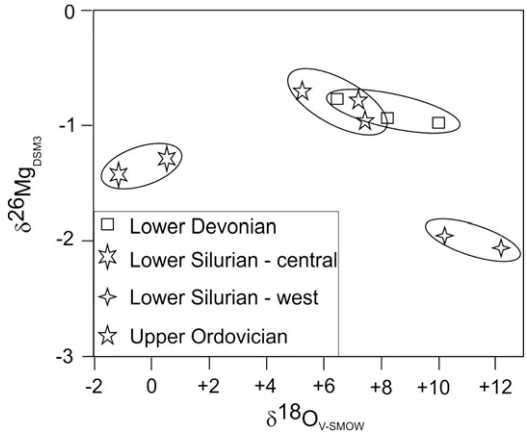

Fig. 7. $\delta^{26}Mg_{DSM3}$ in saddle dolomite *versus* $\delta^{18}O_{SMOW}$ values of hydrothermal fluids. Data in Table 2.

Gaspé Peninsula and the Lower Devonian sample have Sr-isotope ratios close to their coeval seawater ratios (Fig. 8) and they also have similar $\delta^{26}Mg_{DSM3}$ values. Upper Ordovician dolomites, on the other hand, have more radiogenic $^{87}Sr/^{86}Sr$ ratios compared to coeval seawater, their $\delta^{26}Mg_{DSM3}$ values are slightly less negative compared to the values of the non-radiogenic Lower Silurian (central Gaspé) and Lower Devonian samples.

7. Discussion

7.1. Mg-isotope fractionation at high temperature

Li et al. (2012) provides a Mg isotope fractionation equation for Mg-calcite over the range of 4 to 45 °C, but it is unlikely that this applies to high-temperatures of hydrothermal dolomitization. No experimental data on high temperature (>100 °C) Mg-isotope fractionation in dolomite have been published.

On the basis of empirical data, Geske et al. (2012) suggest that little Mg-isotope fractionation occurs in rock buffered systems at higher temperatures (100–350 °C), suggesting that original marine $\delta^{26}Mg$ values might be preserved in high temperature dolomite. Similarly, Azmy et al. (2013) showed a slight enrichment in $\delta^{26}Mg$ from early (30 °C) to late burial (153 °C) replacement dolomites albeit with largely overlapping $\delta^{26}Mg$ values. Kinetic fractionation of the Mg-isotopes does not control the $\delta^{26}Mg$ values of the replacement dolomites in the interpreted semi-closed diagenetic system.

7.2. Diagenetic fluids and Mg-isotopes

The hydrothermal fluids responsible for the precipitation of these saddle dolomites likely originated from different sources. The Upper Ordovician dolostones are associated with faults rooted in the crystalline Precambrian basement (Lavoie et al., 2005; Lavoie and Chi, 2010) whereas the Lower Silurian and Lower Devonian dolostones occur at faulted contacts, or near Ordovician mafic and ultramafic units as well as close to Devonian intrusives (Pinet et al., 2008; Lavoie and Chi, 2010; Lavoie et al., 2010).

Lower Silurian Sayabec dolomites (Fig. 5) exhibit an interesting Mg-isotope relation, the higher temperature (average $T_h = 175$ °C) dolomite in western Gaspé (Tables 1 and 2, Fig. 5) has more negative $\delta^{26}Mg_{DSM3}$ values (−2.09 and −1.91‰) than the lower temperature (average T_h of 153 °C) dolomite of central Gaspé (−1.41 to −1.13‰). This difference in $\delta^{26}Mg_{DSM3}$ values is also suggested by the different values of $\delta^{18}O_{VSMOW}$ of the diagenetic fluid (Table 2, Fig. 2). Both Gaspé dolomitized geobodies are in faulted contact with Ordovician ultramafic complexes that were suggested to be a source of Mg^{+2} for dolomitization (Lavoie and Morin, 2004; Lavoie and Chi, 2010). The difference in their $\delta^{26}Mg_{DSM3}$ values might be related to distinct sources of Mg^{+2} or could indicate a similar original fluid that went through multiple rock–water exchanges and/or mixing with a different fluid.

The diagenetic conditions that prevailed at the time of precipitation of these lower Paleozoic pore-filling saddle dolomites were likely different from those documented in the replacement dolomites (early dolomicrite to late saddle dolomite) of the Triassic and Lower Ordovician by Geske et al. (2012) and Azmy et al. (2013). From the latter two studies, Mg fractionation would be relatively small and the $\delta^{26}Mg_{DSM3}$ values of saddle dolomites should be close to that of the

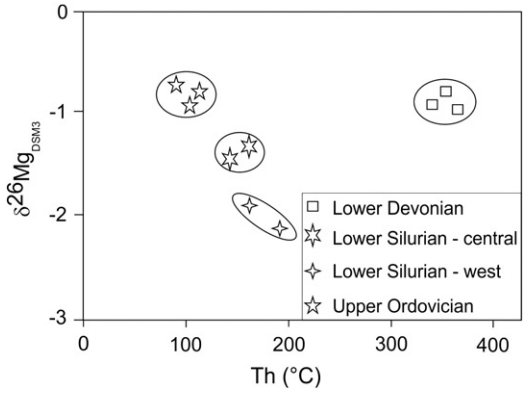

Fig. 6. $\delta^{26}Mg_{DSM3}$ *versus* fluid inclusion homogenization temperatures (T_h) in saddle dolomite cements. Data in Table 2.

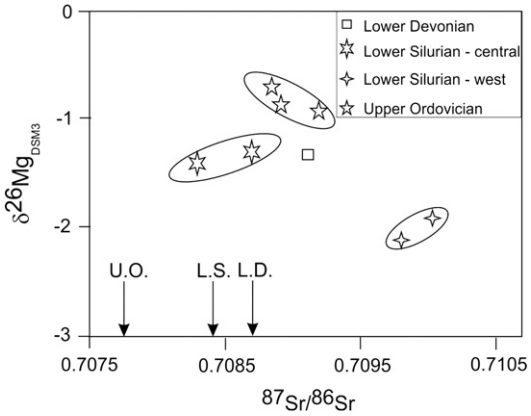

Fig. 8. $\delta^{26}Mg_{DSM3}$ *versus* $^{87}Sr/^{86}Sr$ values in saddle dolomite cements. Marine $^{87}Sr/^{86}Sr$ values are shown for Upper Ordovician (U.O.), Lower Silurian (L.S.) and Lower Devonian (L.D.). Data in Table 2.

high-temperature fluid from which they precipitated. However, even for the open diagenetic system assumed for the herein cases, the chemical evolution of diagenetic fluids prior to dolomite precipitation is largely unknown.

7.3. Mg-isotopes and source of Mg

One critical aspect for the applicability of Mg isotope geochemistry in the understanding of the dolomites resides in the capacity to use δMg_{DSM3} to generate information on the source of diagenetic fluid Mg^{+2}. Obviously, δMg_{DSM3} data will have to be integrated into an overall complete conventional field-diagenetic study of the dolostone. The δMg_{DSM3} values in dolomite cement are assumed to be primarily controlled by the isotopic composition of the diagenetic fluid that possibly carries Mg^{+2} from various sources.

The important volume of dolostones in the Lower Paleozoic rocks of eastern Canada implies that significant sources of Mg were available. Based on the various types of dolostones, including facies-controlled to fault-controlled dolostone bodies, more than a single dolomitization model can be postulated. In order to test the applicability of Mg-isotopes as a useful new research tool for understanding dolomitization processes, we have restricted our initial analyses to fault-controlled dolostone bodies with geochemical and petrographical data supportive of dolomitization temperatures higher than maximum burial temperatures recorded by these successions.

The most likely significant sources of Mg are marine waters, Mg recycled from precursor carbonates, post-evaporite and deep basinal brines, shales, and mafic to ultramafic igneous units. Available literature on Mg-isotopes in these types of potential source rocks suggests that significant isotopic differences exist among them (Wombacher et al., 2009). In the lower Paleozoic succession considered here, no significant evaporite deposits are known and a source associated with post-evaporite brine is not considered. Moreover, there are almost no available data on fractionation factors between mineral sources of Mg^{+2} and diagenetic fluids at low and high temperatures.

7.3.1. Marine water and recycled marine carbonates

Magnesium is the fourth most abundant ion in marine water (Culkin and Cox, 1966; Millero, 1974). Modern seawater has a fairly uniform $\delta^{26}Mg_{DSM3}$ value of −0.8‰ (Young and Galy, 2004; Teng et al., 2010). Based on Mg/Ca ratios of marine waters, marine carbonates will incorporate some Mg in their crystal lattice, forming low to high Mg-calcite. Under specific conditions, synsedimentary dolomite can be formed from seawater (Morse and MacKenzie, 1990), a process that is catalysed by bacteria (van Lith et al., 2002; Krause et al., 2012; Zhang et al., 2013). The low and high Mg-calcites from marine waters can be recycled and be a source of Mg^{+2} for later dolomitization. Modern biogenic marine calcite shows a significant taxon-dependent fractionation of Mg-isotopes with $\delta^{26}Mg_{DSM3}$ values ranging from −5.0 to −1.0‰ (Hippler et al., 2009; Azmy et al., 2013). Li et al. (2012) documented small thermal isotopic fractionation between Mg-saturated water and inorganically precipitated Mg-calcite from controlled experiments between 4 and 45 °C. Phanerozoic limestones and dolostones show a wide range of $\delta^{26}Mg_{DSM3}$ values, ranging from −5.0 to −1.0‰, with dolostones yielding isotopic values in the heavy end of the range (−2.5 to −1.0‰, Brenot et al., 2008; Immenhauser et al., 2010).

Limestones and dolostones are abundant in the Lower Paleozoic successions of eastern Canada (Lavoie, 2008) and their importance as a potential source of Mg^{+2} has to be considered, especially in the case of replacement dolomitization.

7.3.2. Shales

Some phyllosilicates are complex Mg-bearing minerals and their original mineralogy depends on multiple factors that include the composition of the parent source rock and the climatic conditions at the time of weathering. There are limited $\delta^{26}Mg_{DSM3}$ values available for modern and ancient marine shales. Analyses of modern clays derived from tropical volcanic soils indicate that all clay fractions have $\delta^{26}Mg_{DSM3}$ values ranging from −0.41 ± 0.04‰ to −0.10 ± 0.08‰, and are isotopically slightly heavier than their parent andesite (−0.47 ± 0.09‰; Opfergelt et al., 2012). Wombacher et al. (2009) indicate that marine muds have $\delta^{26}Mg_{DSM3}$ values of −0.26 ± 0.09‰. Li et al. (2010) have analysed "post-archean" (Proterozoic to Cretaceous) shales in Australia; these have yielded $\delta^{26}Mg_{DSM3}$ values ranging from −0.27 ± 0.08‰ to +0.49 ± 0.07‰.

7.3.3. Mafic and ultramafic volcanics

Magnesium-rich minerals (chlorite, pyroxene, hornblende, and forsterite–olivine, among others) are abundant in mafic and ultramafic volcanic units. These minerals are highly reactive and will release Mg^{+2} during high and low temperature alteration of the hosts. Analyses of modern mid-ocean ridge basalts (MORB) and ancient peridotites (Teng et al., 2010) have yielded very similar $\delta^{26}Mg_{DSM3}$ values of −0.26 ± 0.07‰ and −0.25 ± 0.04‰, respectively.

7.3.4. Considerations of Mg sources in the Lower Paleozoic of eastern Canada

The δMg_{DSM3} signatures of high temperature saddle dolomite cements from the Lower Paleozoic indicate differences in the Mg-isotope composition of the fluid responsible for dolomite precipitation. This assertion is also supported by the relationship between δMg_{DSM3} in the saddle dolomites and $\delta^{18}O_{VSMOW}$ of the fluids, which indicate that diverse diagenetic fluids had potentially different Mg-isotope compositions. These elements suggest that the ultimate source of the Mg-isotope in the fluid could eventually be fingerprinted using the δMg_{DSM3} signatures of the high temperature saddle dolomites.

Preliminary work on Mg-isotope values on potential Mg source rocks in the successions covered by our study indicates significant variations of the δMg_{DSM3} signatures between lower Paleozoic shales and volcanic rocks (work in progress). However, for these old rocks, it is likely that they have lost their initial δMg_{DSM3} values through either early burial thermal maturation and/or clay alteration for the shales and through various alteration and/or metasomatic processes for the volcanic rocks.

The recognition of a specific source of Mg^{+2} in the diagenetic fluid from the δMg_{DSM3} values in saddle dolomite could provide an additional argument to evaluate the likelihood of specific dolomitization models in any given succession. The applicability of Mg-isotopes to provide useful information on dolomitizing fluid and very general ideas about source(s) of magnesium will eventually require the experimental evaluation fractionation factors for dolomite at high temperatures.

8. Conclusions

Research on the use of Mg-isotopes in the field of carbonate diagenesis in general and, more specifically, on the dolomite Mg source problem is in its early days. This contribution presents the first results of Mg-isotope data for fracture- and void-filling, paragenetically and geochemically well-controlled hydrothermal saddle dolomites in Lower Paleozoic successions. This study is restricted to saddle dolomite cements in order to evaluate the usefulness of Mg-isotopes for high water/rock ratio diagenetic settings. Saddle dolomites in Upper Ordovician, Lower Silurian and Lower Devonian hydrothermal dolostones occur over diverse geological basements. These three different cases of hydrothermal dolomitization recorded, based on fluid inclusion microthermometry, precipitation temperatures above maximum burial temperatures.

The $\delta^{26}Mg_{DSM3}$ values for Upper Ordovician samples (N = 5) range from −1.26 to −0.71‰, from −3.25 to −1.13‰ for Lower Silurian samples (N = 7) and from −1.29 to −0.78‰ for Lower Devonian samples (N = 4). From the microthermometric (T_h) fluid inclusion data, the saddle dolomites likely did not precipitated out of a unique fluid as the lower temperature Upper Ordovician case (T_h of 102 °C) has $\delta^{26}Mg_{DSM3}$ values statistically similar to those of the high

temperature Lower Devonian case (T_h of 350 °C). The same applies to the Lower Silurian cases of the Sayabec Formation where two domains are recognized based of T_h values (152 and 175 °C, for central and western Gaspé peninsula, respectively) with the higher temperature cases having the more negative $\delta^{26}Mg_{DSM3}$ values.

Based on conventional isotopes ($\delta^{18}O_{VPDB}$ and $\delta^{18}O_{VSMOW}$ for dolomite–fluid and $\delta^{13}C_{VPDB}$ and $^{87}Sr/^{86}Sr$ of dolomite) and fluid inclusion microthermometry (T_h and salinity), it has been shown in previous studies that the high temperature dolomitization for these three cases proceeded from different diagenetic fluids. This interpretation is supported by the new Mg-isotope data from the saddle dolomites. The Lower Silurian cases are significant for that aspect, the conventional research approach suggested that different dolomite-rich fluids were present for central and western Gaspé occurrences; an assertion backed by the $\delta^{26}Mg_{DSM3}$ values of the saddle dolomites.

Mg-isotope characterization of potential sources of Mg^{+2} in the Lower Paleozoic successions of eastern Canada is in progress and preliminary data indicate statistically significant differences between potential Mg sources. Experimental research is needed in order to constraint the fractionation factors between diagenetic fluids and various Mg-rich minerals in order for Mg-isotope to develop as an eventual critical tool to address the major issue of Mg-source for any given burial dolomitization model.

Acknowledgements

The authors would like to thank M.M. Savard for her review of the initial draft of this manuscript; thanks are also expressed to A. Geske, A. Immenhauser, B. Goldstein and H. Chafetz for commenting on an earlier draft of this contribution. The manuscript benefited from the much appreciated review of A. Immenhauser. Many fruitful discussions with colleagues over the years have been instrumental in the development of the hydrothermal model for some Lower Paleozoic dolostones in eastern Canada, particularly thanks to G. Chi, K. Azmy, M. M. Savard, L. Smith and G. Davies. This is Geological Survey of Canada Contribution 20120311.

References

Azmy, K., Lavoie, D., Wang, Z., Brand, U., Al-Aasm, I., Jackson, S., Girard, I., 2013. Magnesium-isotope and REE compositions of Lower Ordovician carbonates from eastern Laurentia: implications for the origin of dolomites and limestones. Chemical Geology 356, 64–75.

Bourque, P.-A., Amyot, G., Desrochers, A., Gignac, H., Gosselin, C., Lachambre, G., Laliberté, J.Y., 1986. Silurian and Lower Devonian reef and carbonate complexes of the Gaspé Basin, Québec — a summary. Bulletin of Canadian Petroleum Geology 34, 452–489.

Braithwaite, C.J.R., Rizzi, G., Darke, G., 2004. The Geometry and Petrogenesis of Dolomite Hydrocarbon Reservoirs: an Introduction. In: Braithwaite, C.J.R., Rizzi, G., Darke, G. (Eds.), Geological Society of London, Special Publication, 235, pp. 1–6.

Brenot, A., Cloquet, C., Vigier, N., Carignan, J., France-Lanord, C., 2008. Magnesium isotope systematics of the lithologically varied Moselle river basin, France. Geochimica et Cosmochimica Acta 72, 5070–5089.

Conliffe, J., Azmy, K., Knight, I., Lavoie, D., 2009. Dolomitization in the Lower Ordovician Watts Bight Formation of the St Georges Group, Western Newfoundland. Canadian Journal of Earth Sciences 46, 247–261.

Conliffe, J., Azmy, K., Gleeson, S.A., Lavoie, D., 2010. Fluids associated with hydrothermal dolomitization in St. George Group, western Newfoundland, Canada. Geofluids 10, 422–437.

Culkin, F., Cox, R.A., 1966. Sodium, potassium, magnesium, calcium and strontium in sea water. Deep-Sea Research 3, 789–804.

Davies, G.R., Smith, L.B., 2006. Structurally controlled hydrothermal dolomite reservoir facies: an overview. Bulletin of American Association of Petroleum Geologists 90, 1641–1690.

de Dolomieu, D., 1791. Sur un genre de pierres calcaires très peu effervescentes avec les acides et phosphorescentes par la collision. Journal de Physique 39, 3–10.

Denison, R.E., Koepnick, R.B., Burke, W.H., Hetherington, E.A., Fletcher, A., 1997. Construction of the Silurian–Devonian seawater $^{87}Sr/^{86}Sr$ curve. Chemical Geology 140, 109–121.

Galy, A., Belshaw, N.S., Halicz, L., O'Nions, R.K., 2001. High precision measurement of magnesium isotopes by multiple-collector inductively coupled plasma mass spectrometry. International Journal of Mass Spectrometry 208, 89–98.

Galy, A., Yoffe, O., Janney, P.E., Williams, R.W., Cloquet, C., Alard, O., Halicz, L., Wadhwa, M., Hutcheon, I.D., Ramon, E., Carignan, J., 2003. Magnesium isotope heterogeneity of the isotopic standard SRM 980 and new reference materials for magnesium isotope ratio measurements. Journal of Analytical Atomic Spectrometry 18, 1352–1356.

Geske, A., Zorlu, J., Richter, D.K., Buhl, D., Niedermayr, A., Immenhauser, A., 2012. Impact of diagenesis and low grade metamorphosis on isotope ($\delta^{26}Mg$, $\delta^{13}C$, $\delta^{18}O$ and $^{87}Sr/^{86}Sr$) and elemental (Ca, Mg, Mn, Fe, and Sr) signatures of Triassic sabkha dolomites. Chemical Geology 332–333, 45–64.

Higgins, J.A., Schrag, D.P., 2010. Constraining magnesium cycling in marine sediments using magnesium isotopes. Geochimica et Cosmochimica Acta 74, 5039–5053.

Hippler, D., Buhl, D., Witbaard, R., Richter, D.K., Immenhauser, A., 2009. Towards a better understanding of magnesium-isotope ratios from marine skeletal carbonates. Geochimica et Cosmochimica Acta 73, 6134–6146.

Hsu, K.J., 1966. The origin of dolomite in sedimentary sequences: a critical analysis. Mineralium Deposita 2, 133–138.

Humphrey, J.D., Quinn, T.M., 1989. Coastal mixing zone dolomite, forward modeling, and massive dolomitization of platform-margin carbonates. Journal of Sedimentary Research 59, 438–454.

Humphrey, J.D., Quinn, T.M., 1990. Coastal mixing zone dolomite, forward modeling, and massive dolomitization of platform-margin carbonates — reply. Journal of Sedimentary Research 60, 3–1016.

Hurley, N.F., Budros, R., 1990. Albion-Scipio and Stoney Point fields — USA Michigan Basin. In: Beaumont, E.A., Foster, N.H. (Eds.), Stratigraphic Traps. , 1. American Association of Petroleum Geologists, Treaty of Petroleum Geology, Atlas of Oil and Gas fields, pp. 1–38.

Immenhauser, A., Buhl, D., Richter, D., Niedermayr, A., Riechelmann, D., Dietzel, M., Schulte, U., 2010. Magnesium-isotope fractionation during low-Mg calcite precipitation in a limestone cave — field study and experiments. Geochimica et Cosmochimica Acta 74, 4346–4364.

Jones, D.G., Xiao, Y., 2005. Dolomitization, anhydrite cementation, and porosity evolution in a reflux system: insights from reactive transport models. Bulletin of American Association of Petroleum Geologists 89, 577–601.

Krause, S., Liebetrau, V., Gorb, S., Sánchez-Román, M., McKenzie, J.A., Treude, T., 2012. Microbial nucleation of Mg-rich dolomite in exopolymeric substances under anoxic modern seawater salinity: new insight into an old enigma. Geology 40, 587–590.

Lavoie, D., 2008. Appalachian foreland basin of Canada. In: Miall, A.D. (Ed.), Sedimentary Basins of the World — USA and Canada. Elsevier Science, pp. 65–103.

Lavoie, D., Chi, G., 2001. The Lower Silurian Sayabec Formation in northern Gaspé: carbonate diagenesis and reservoir potential. Bulletin of Canadian Petroleum Geology 49, 282–298.

Lavoie, D., Chi, G., 2006. Hydrothermal dolomitization in the Lower Silurian La Vieille Formation in northern New Brunswick: geological context and significance for hydrocarbon exploration. Bulletin of Canadian Petroleum Geology 54, 380–395.

Lavoie, D., Chi, G., 2010. Lower Paleozoic foreland basins in eastern Canada: tectono-thermal events recorded by faults, fluids and hydrothermal dolomites. Bulletin of Canadian Petroleum Geology 58, 17–35.

Lavoie, D., Morin, C., 2004. Hydrothermal dolomitization in the Lower Silurian Sayabec Formation in northern Gaspe — Matapedia (Quebec): first constraint on timing of porosity and regional significance for hydrocarbon reservoirs. Bulletin of Canadian Petroleum Geology 52, 256–269.

Lavoie, D., Chi, G., Brennan-Alpert, P., Desrochers, A., Bertrand, R., 2005. Hydrothermal dolomitization in the Lower Ordovician Romaine Formation of the Anticosti Basin: significance for hydrocarbon exploration. Bulletin of Canadian Petroleum Geology 52, 454–472.

Lavoie, D., Pinet, N., Dietrich, J., Hannigan, P., Castonguay, S., Hamblin, A.P., Giles, P.S., 2009. Petroleum resource assessment, Paleozoic succession of the St. Lawrence Platform and Appalachians of eastern Canada. Geological Survey of Canada, Open File report 6174 (275 pp.).

Lavoie, D., Chi, G., Urbatsch, M., Davis, B., 2010. Massive dolomitization of a pinnacle reef in the lower Devonian West Point Formation (Gaspé Peninsula, Québec) — an extreme case of hydrothermal dolomitization through fault-focussed circulation of magmatic fluids. American Association of Petroleum Geologists 94, 513–531.

Lavoie, D., Zhang, S., Pinet, N., 2011. Hydrothermal dolomites in Hudson Bay Platform and southeast Arctic Platform: preliminary field and geochemical data. Geological Survey of Canada, Open File report 7002 (19 pp.).

Li, W.-Y., Teng, F.-Z., Ke, S., Rudnick, R.L., Gao, S., Wu, F.-Y., Chappel, B.W., 2010. Heterogeneous magnesium isotopic composition of the upper continental crusts. Geochimica et Cosmochimica Acta 74, 6867–6884.

Li, W.-Y., Chakraborty, S., Beard, B.L., Romanek, C.S., Johnson, V.M., 2012. Magnesium isotope fractionation during precipitation of inorganic calcite under laboratory conditions. Earth and Planetary Science Letters 333–334, 304–316.

Machel, H.G., 1987. Saddle dolomite as a by-product of chemical compaction and thermochemical sulphate reduction. Geology 15, 936–940.

Machel, H.G., 2004. Concepts and models of dolomitization: a critical reappraisal. In: Braithwaite, C.J.R., Rizzi, G., Darke, G. (Eds.), The geometry and petrogenesis of dolomite hydrocarbon reservoirs. Geological Society of London, Special Publication, 235, pp. 7–63.

Machel, H.G., Mountjoy, E.W., 1986. Chemistry and environments of dolomitization — a reappraisal. Earth Science Reviews 23, 175–222.

Machel, H.G., Mountjoy, E.W., 1990. Coastal mixing zone dolomite, forward modelling, and massive dolomitization of platform-margin carbonate — discussion. Journal of Sedimentary Petrology 60, 1008–1012.

Mavromatis, V., Gautier, Q., Bosc, O., Schott, J., 2013. Kinetics of Mg partition and Mg stable isotope fractionation during its incorporation in calcite. Geochimica et Cosmochimica Acta 114, 188–203.

Millero, F.J., 1974. The physical chemistry of seawater. Annual Review of Earth and Planetary Sciences 2, 101–150.

Morse, J.W., MacKenzie, F.T., 1990. Geochemistry of Sedimentary Carbonates. Elsevier, Amsterdam (707 pp.).
Opfergelt, S., Georg, R.B., Delvaux, B., Cabidoche, Y.-M., Burton, K.W., Halliday, A.N., 2012. Mechanisms of magnesium isotope fractionation in volcanic soil weathering sequences, Guadeloupe. Earth and Planetary Science Letters 341–344, 176–185.
Pinet, N., Lavoie, D., Keating, P., Brouillette, P., 2008. Gaspé belt subsurface geometry in the northern Québec Appalachians as revealed by an integrated geophysical and geological study. 1 — potential field mapping. Tectonophysics 460, 34–54.
Shields, G.A., Carden, G.A.F., Veizer, J., Meidla, T., Rong, J.-Y., Li, R.-Y., 2003. Sr, C and O isotope geochemistry of Ordovician brachiopods: a major isotopic event around the Middle–Late Ordovician transition. Geochimica et Cosmochimica Acta 67, 2005–2025.
Sibley, D.F., Greg, J.M., 1987. Classification of dolomite rock textures. Journal of Sedimentary Petrology 57, 967–975.
Teng, F.A., Li, W.-Y., Ke, S., Marty, B., Dauphais, N., Huang, S., Wu, F.-Y., Pourrmand, A., 2010. Magnesium isotope composition of the Earth and chondrites. Geochimica et Cosmochimica Acta 74, 4150–4166.
van Lith, Y., Vasconcelos, C., Warthmann, R., Martins, J.C.F., McKenzie, J.A., 2002. Bacterial sulphate reduction and salinity: two controls on dolomite precipitation in Lagoa Vermelha and Brejo do Espino (Brazil). Hydrobiologia 485, 35–59.
van Tuyl, F.M., 1914. The origin of dolomite. Annual Report AR-25C. Iowa Geological Survey 25, 251–422.
Wombacher, F., Eisenhauer, A., Heuserac, A., Weyer, S., 2009. Separation of Mg, Ca and Fe from geological reference materials for stable isotope ratio analyses by MC-ICP-MS and double-spike TIMS. Journal of Analytical Atomic Spectrometry 24, 627–636.
Young, E.D., Galy, A., 2004. The isotope geochemistry and cosmochemistry of magnesium. Reviews in Mineralogy and Geochemistry 55, 197–230.
Zhang, F., Yan, C., Teng, H.H., Roden, E.E., Xu, H., 2013. *In situ* AFM observations of Ca–Mg carbonate crystallization catalyzed by dissolved sulphide: implications for sedimentary dolomite formation. Geochimica et Cosmochimica Acta 105, 44–55.
Zheng, Y.-F., 1999. Oxygen isotope fractionation in carbonate and sulfate minerals. Geochemical Journal 33, 109–126.